Tectonophysics 586 (2013) 1–14

Contents lists available at SciVerse ScienceDirect

Tectonophysics

journal homepage: www.elsevier.com/locate/tecto

Large, pre-digital earthquakes of the Bonin-Mariana subduction zone, 1930–1974

Emile A. Okal [a,*], Dominique Reymond [b], Sutatcha Hongsresawat [a,1]

[a] Department of Earth and Planetary Sciences, Northwestern University, Evanston, IL 60208, USA
[b] Laboratoire de Géophysique, Commissariat à l'Energie Atomique, Boîte Postale 640, 98713 Papeete, Tahiti, French Polynesia

ARTICLE INFO

Article history:
Received 14 March 2012
Received in revised form 23 August 2012
Accepted 8 September 2012
Available online 17 September 2012

Keywords:
Historical earthquakes
Decoupled subduction zones
Bonin Islands
Mariana Islands

ABSTRACT

The Bonin-Mariana subduction zone is the end-member example of a decoupled system, as described by Uyeda and Kanamori (1979), with no interplate thrust solutions of moments greater than 8×10^{25} dyn cm known in the CMT catalog, although a number of earthquakes are reported with assigned magnitudes around or above 7, both during the WWSSN period and the historical pre-1962 era. We present a systematic study of these events, including relocation and inversion of moment tensors. We obtain 15 new moment tensor solutions, featuring a wide variety of focal mechanisms both in the fore-arc and the outer rise, and most importantly a shallow-dipping interplate thrust mechanism with a moment of 4×10^{27} dyn cm for the event of 28 December 1940 at a location 175 km East of Pagan. Our results show that the modern CMT catalog still undersamples the seismicity of the Mariana arc, which is thus not immune to relatively large, albeit rare, interplate thrust events, with moments 40 times that of the largest Global-CMT solution. Frequency-magnitude relations would then suggest a return time of 320 years for a magnitude 8 interplate thrust faulting earthquake in the Bonin-Mariana system.

Contents

1. Introduction and background

One of the most important scientific lessons from the 2004 Sumatra and 2011 Tohoku disasters has been that the maximum earthquake expectable in a subduction zone does not correlate easily with simple tectonic parameters. It had been suggested (Ruff and Kanamori, 1980) that a combination of plate youth and spreading

* Corresponding author. Fax: +1 847 491 8060.
E-mail address: emile@earth.northwestern.edu (E.A. Okal).
[1] Present address: Department of Geological Sciences, University of Florida, Gainesville, FL 32611, USA.

0040-1951/$ – see front matter © 2012 Elsevier B.V. All rights reserved.
http://dx.doi.org/10.1016/j.tecto.2012.09.006

rate could characterize the seismic potential of a given region for great or mega events, namely that the latter occurred only in zones such as Central Chile, where young oceanic lithosphere subducts at a fast rate. Under that model, the North Sumatra trench should not have generated events with moments greater than 3×10^{28} dyn cm, in rough numbers 30 times less than that of the 2004 earthquake (Stein and Okal, 2005; Tsai et al., 2005). While the 1964 Alaska event did violate Ruff and Kanamori's (1980) paradigm, it was regarded at the time as an acceptable "exception confirming the rule," with still 80% of the observed maximum earthquakes accurately predicted by the model (Ruff and Kanamori, 1983). The combination of newly occurring or discovered events (Sumatra, 2004; Cascadia, 1700), and of a critical reassessment of the relevant tectonic and seismological data led Stein and Okal (2007) to revise this figure down to 35%, at which point the model is no longer satisfactory. The recent 2011 Tohoku earthquake is another clear violator, as it took place in lithosphere aged ~135 Ma, and converging at an average rate of 7.3 cm/yr (Müller et al., 1997; Sella et al., 2002). Its moment (4×10^{29} dyn cm) exceeded that predicted by Ruff and Kanamori's (1980) model by a factor of at least 10.

Following a different approach, Ruff (1989) had suggested that the level of sedimentation at subduction interfaces could be a controlling factor of the size of maximum earthquakes, an idea later pursued by Scholl et al. (2007, 2010), but careful reassessment of critical events, such as the 1952 Kamchatka, 1877 Northern Chile, 1868 Southern Peru and 2011 Tohoku earthquakes, shows that this potential correlation again suffers too many exceptions to be significant, and especially to be used confidently for the estimation of seismic and tsunami risk (Okal et al., 2006; Stein and Okal, 2007).

Rather, a precautionary approach now dictates that any subduction zone should be regarded as carrying the potential for a mega rupture, limited only by the total length of the available subduction system (McCaffrey, 2007; Stein and Okal, 2007).

In this context, the Bonin-Mariana subduction zone (Fig. 1a), where Pacific lithosphere aged 140–150 Ma subducts at 3–4 cm/yr (Müller et al., 1997; Sella et al., 2002), has long been considered an endmember to any classification of subduction zones according to their degree of coupling (Uyeda and Kanamori, 1979). In addition to featuring the deepest known oceanic trenches, an essentially vertical Wadati–Benioff zone, and vigorous back-arc spreading and trench migration, it is characterized by a total lack of documented great interplate thrust earthquakes, the largest known such event in the CMT catalog being the earthquake of 26 May 1978 in the Volcano Islands ($M_0=8.2\times10^{25}$dyn cm; gray star on Fig. 1).

In their landmark study, Ruff and Kanamori (1980) had used a maximum magnitude $M=7.2$ for the Marianas, reflecting a number of events listed by Gutenberg and Richter (1954; hereafter GR), actually reaching $M_{PAS}=7.3$ on 24 February 1934. However, these historical earthquakes remain poorly known since, to our knowledge, they have not been studied with modern techniques. In particular, their focal mechanisms are not available, and they may not represent an interplate motion between the Pacific and Philippine plates, as in the case of other "decoupled" subduction zones, where the largest known earthquakes have been found to express normal faulting or tears inside the subducting plate (Okal and Hartnady, 2009; Stein et al., 1982). Indeed, the largest known CMT solution in the Bonin-Marianas is the normal faulting outer rise earthquake of 21 December 2010 ($M_0=1.8\times10^{27}$dyn cm), with a comparable event ($M_0=1.6\times10^{27}$dyn cm) on 05 April 1990 in the Southern Marianas (open stars on Fig. 1).

In the present paper, we conduct a systematic study of these historical earthquakes, including relocation and seismic moment tensor inversion. We obtain 15 new moment tensor solutions and conclude that, while the majority of these sources involve normal faulting, at least four of them feature thrust mechanisms in environments where they could represent interplate motion, at significantly higher seismic moments than documented during the digital (post-1976) era.

2. Data set and methodologies

We initially targeted for study events occurring between 1910 and 1975, with at least one reported magnitude greater than 7, catalog hypocenters between latitudes 14°N and 30°N, longitudes 140°E and 149°E, and shallower than 100 km. For earthquakes post-dating 1962, we lowered these thresholds to $h<70$ km; $m_b\geq6$, since the availability of the WWSSN allows waveform modeling of smaller sources, and catalog hypocentral depths are expected to be more accurate. This initial dataset comprises a mere 16 events, of which only 3 are located North of 23°N, in the Volcano–Bonin section of the subduction system. Since our purpose is to assess the largest historical earthquakes, we then lowered the magnitude threshold to any magnitude greater than 6.5 in that specific region. Despite an intermediate cataloged depth (110 km), we also include in our dataset the earthquake of 24 November 1914, because of its exceptional magnitude (8.7), as compiled in the NOAA geophysical database. The final dataset comprises 24 earthquakes, listed in Tables 1 and 2.

2.1. Relocation

For events before 1963, relocations were performed from the datasets of arrival times compiled in the International Seismological Summary (ISS, later ISC), using the interactive iterative method of

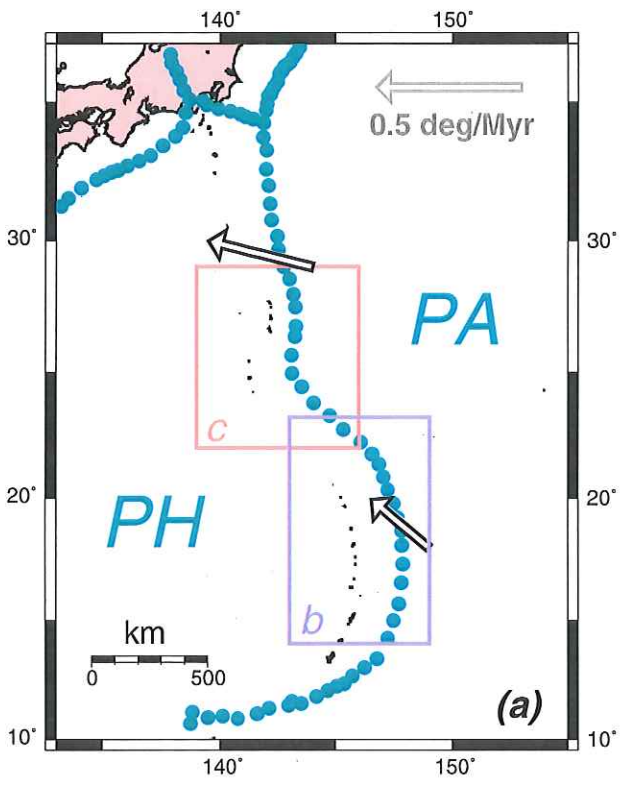

Fig. 1. (a): General map of the study area, showing major plate boundaries (Bird, 2003) and convergence vectors between the Pacific (PA) and Philippines (PH) plates (Sella et al., 2002). The boxes identify the domains of the more detailed maps. Relocations and focal solutions obtained in this study are shown separately for the Mariana Islands (b) and the Bonin Islands (c). Red dots show relocated epicenters, with associated Monte Carlo error ellipses. Triangles refer to unrelocated post-1962 events. Focal mechanisms are color-keyed (blue: normal faulting; red: thrust faulting; green: strike-slip). Bold numbers at right refer to Tables 1–3. Isobaths are shown in blue at 1000-m intervals (magenta for 7000 m and deeper); the 500-m one is in green. The smaller gray symbols refer to the two largest CMT solutions known in the entire Bonin-Mariana system (open stars) and to the largest interplate thrust CMT solution (gray star). The brown dots (with large Monte Carlo ellipses) are the relocated epicenters of the 1913 and 1914 events, most probably of intermediate depths.

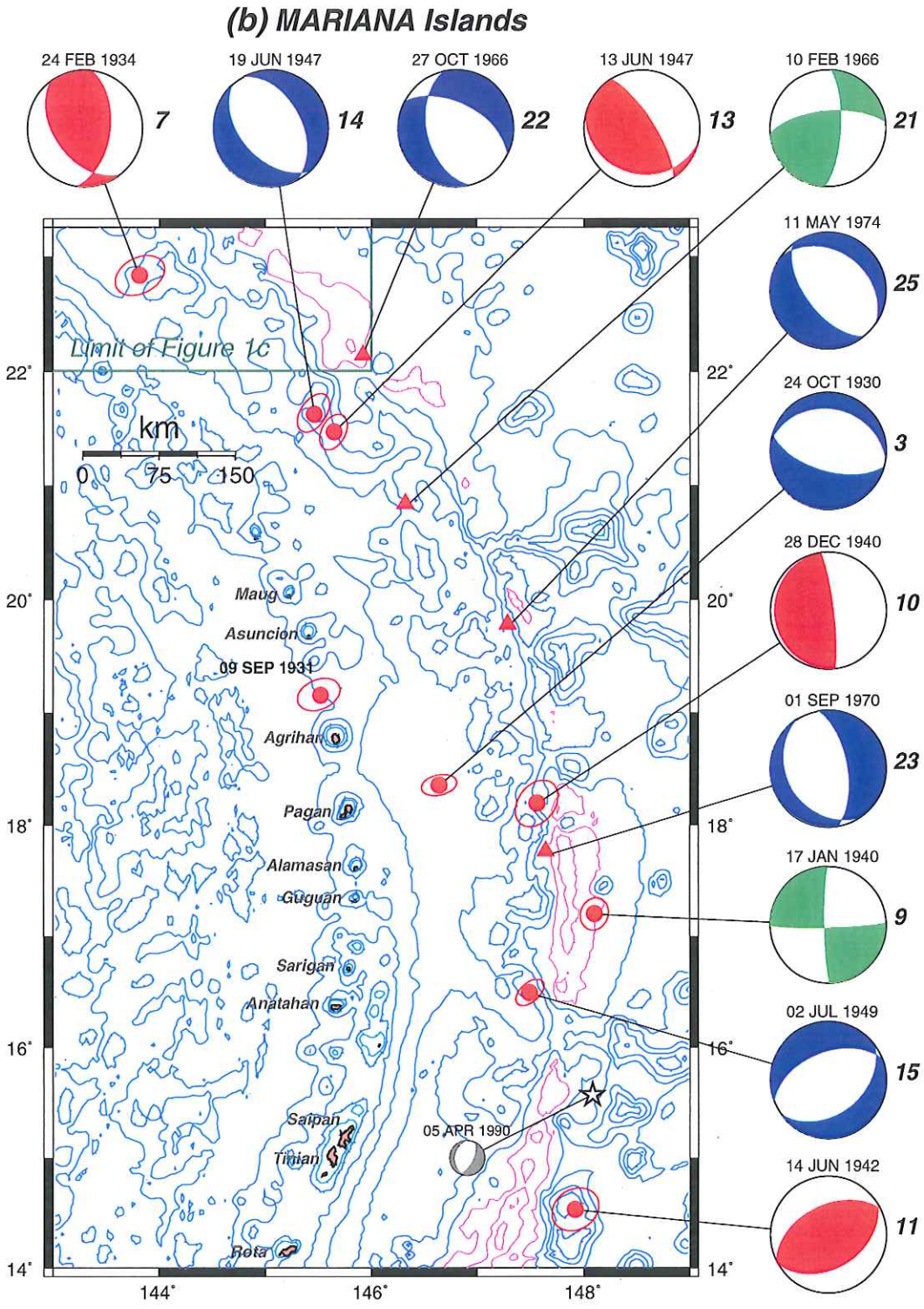

Fig. 1 (*continued*).

Wysession et al. (1991), which includes a Monte Carlo algorithm injecting Gaussian noise into the dataset. The standard deviation σ_G of the noise varies with the epoch of the event from a minimum of 2 s in 1960 to 15 s in the 1910s. In seven instances (flagged by "F" in Table 1), hypocentral depth could be inverted by letting it float during the relocation. Otherwise ("C"), the depth was estimated by minimizing the root-mean-squares residual σ for constrained relocations at depths ranging from 10 to 200 km, as detailed by Rees and Okal (1987).

We did not relocate the events of the WWSSN era (post-1962) and simply list in Table 2 their epicentral parameters as compiled by the ISC, and by Engdahl and Villaseñor (2002, hereafter EV) as part of their Centennial Catalogue.

The results of the relocations are discussed individually for the main "primary" events in Appendix 1. Those "ancillary" earthquakes relocating inside the slab, at or nearly intermediate depths ($h \geq 65$ km), are detailed in Appendix 2. Since this study is concerned with shallow

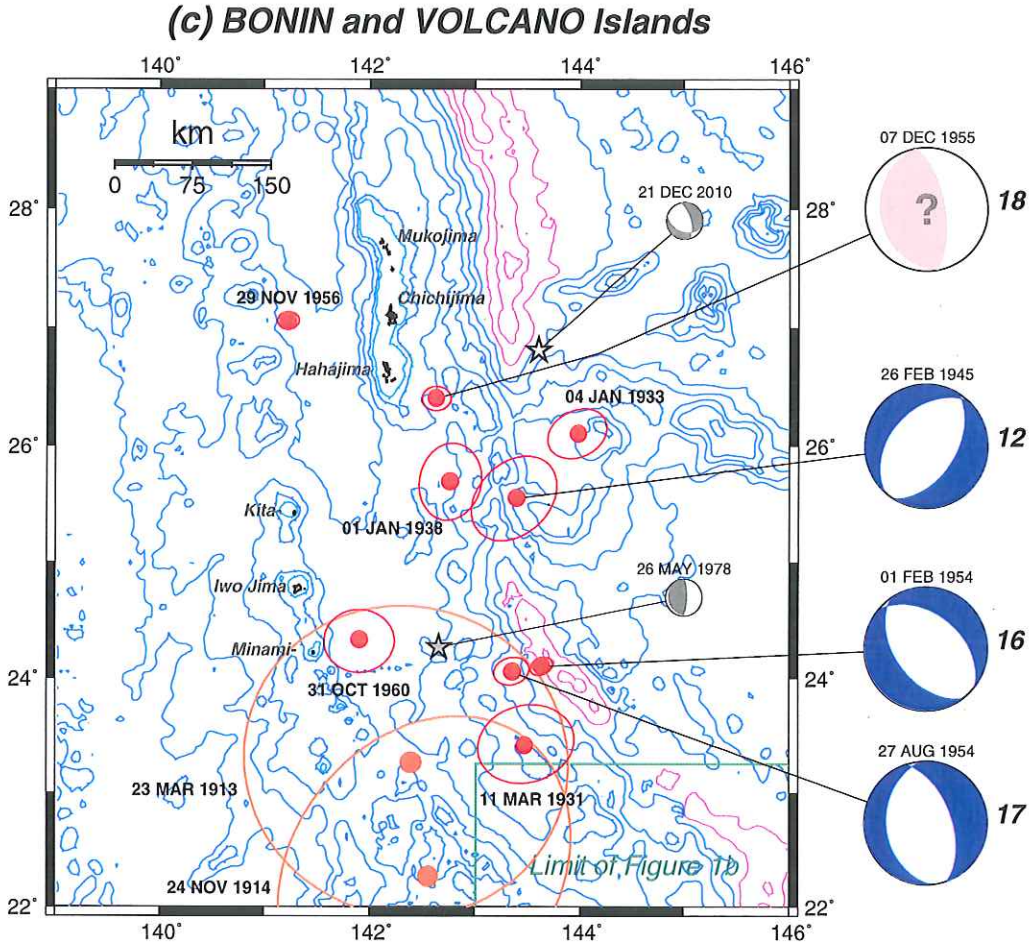

Fig. 1 *(continued).*

Table 1
Historical events (pre-1962) relocated in this study.

Number	Date	Catalog location			Relocation							Magnitude [b]
	D M (J) Y	Lat.	Lon.	Depth	Origin time	Lat.	Lon.	Depth [a]	Stations		σ	
		(°N)	(°E)	(km)	GMT	(°N)	(°E)	(km)	Read	Kept	(s)	
1	23 Mar (082) 1913	24.	142.	80	20:47:29.4	23.28	142.49	150 C	21	19	8.09	7.0 PAS
2	24 Nov (328) 1914	22.	143.	110	11:53:47.8	22.26	142.55	371 F	28	26	5.52	8.1 PAS
3	24 Oct (328) 1930	18.5	147.	0	20:15:09.1	18.35	146.64	15 C	148	140	3.59	7.1 PAS
4	11 Mar (070) 1931	23.	143.5	0	12:26:44.0	23.41	143.47	13 F	65	58	4.30	6¾ PAS
5	09 Sep (252) 1931	19.	145.5	0	20:38:21.6	19.15	145.52	120 C	91	83	2.59	7.1 PAS
6	04 Jan (004) 1933	26.	144	60	01:24:48.4	26.10	143.98	10 C	97	94	3.44	6½ PAS
7	24 Feb (055) 1934	22.5	144.	0	06:23:44.9	22.87	143.80	25 C	139	136	3.49	7.3 PAS
8	01 Jan (001) 1938	25.75	143.	80	23:28:06.3	25.69	142.76	77 F	78	73	2.70	6¾ PAS
9	17 Jan (017) 1940	17.	148.	80	01:14:55.9	17.24	148.12	22 F	92	88	2.85	7.3 PAS
10	28 Dec (363) 1940	18.	147.5	80	16:37:45.1	18.18	147.51	30 C	81	77	2.96	7.3 PAS
11	14 Jun (165) 1942	15.	145	0	03:09:55.5	14.53	147.92	39 F	68	66	2.69	7.0 PAS
12	26 Feb (057) 1945	26.	143.5	50	22:14:24.8	25.55	143.39	10 C	60	53	3.25	7.1 PAS
13	13 Jun (164) 1947	21.5	145.5	0	20:24:51.6	21.47	145.65	10 C	146	146	3.90	7.2 PAS
14	19 Jun (170) 1947	22.	145.5	0	07:34:39.5	21.63	145.46	30 C	121	121	3.28	7.0 PAS
15	02 Jul (183) 1949	16.	148.	50	19:57:12.8	16.49	147.49	10 C	160	160	3.14	7.1 PAS
16	01 Feb (032) 1954	24.	143.	0	01:06:52.9	24.00	143.70	40 C	218	205	3.51	7.1 PAS
17	27 Aug (239) 1954	24.2	143.3	64	10:54:51.5	24.05	143.35	4 F	156	148	3.45	6.7 PAS
18	07 Dec (341) 1955	26.5	143.5	0	15:03:14.3	26.40	142.63	25 C	200	193	3.44	6.9 PAS
19	29 Nov (334) 1956	27.	141.	0	09:15:29.4	27.05	141.22	65 F	211	202	3.30	6¾ PAS
20	31 Oct (305) 1960	24.4	141.8	25	20:50:28.9	24.31	141.89	42 F	14	14	0.87	6.9 BRK

[a] C: constrained; F: floated.
[b] PAS: Reported by Pasadena (Gutenberg and Richter, 1954); BRK: Reported by Berkeley.

Table 2
WWSSN era (1962–1975): events not relocated.

Number	Date	ISC solution				Centenial solution			Magnitudes		
	D M (J) Y	Lat. (°N)	Lon. (°E)	Depth (km)	Origin Time GMT	Lat. (°N)	Lon. (°E)	Depth (km)	m_b	M_s	Other
21	10 Feb (041) 1966	20.73	146.29	29	14:21:09.1	20.76	146.30	42	6.2		6.5 PAS
22	27 Oct (300) 1966	22.11	145.90	44	14:21:06.4	22.14	145.96	9	6.0		
23	01 Sep (244) 1970	17.70	147.65	39	05:11:16.0	17.71	147.70	60	6.3	6.4	6.4 BRK
24	11 May (131) 1974	19.73	147.34	26	06:14:12.0	19.73	147.37	38	6.4	5.9	6.8 PAS

seismicity along, or in the vicinity of, the interplate contact, these earthquakes are not studied further.

2.2. Focal mechanisms and moments

We use different approaches for earthquakes occurring before and after the deployment of the World-Wide Standard Seismological Network (WWSSN).

- WWSSN era (1963–1975)
  During the deployment of the WWSSN network (Events 21–24), the abundance of worldwide high-gain data generally allows the resolution of a focal geometry based on the polarity of *P*-wave first motions. A selection of long-period surface waves can then be used to obtain the scalar moment of the source, by computing mantle magnitudes M_m from Rayleigh and Love waves, using the algorithm of Okal and Talandier (1989), and applying source corrections derived from the body-wave focal solutions, to obtain corrected magnitudes M_c, which are directly related to the seismic moment through

$$log_{10}M_0 = M_c + 20 \quad (1)$$

where M_0 is expressed in dyn cm.

- Pre-WWSSN era
  For events predating 1962, for which the data are scarce, we use the Preliminary Determination of Focal Mechanism (PDFM) as introduced by Reymond and Okal (2000). This method of moment tensor inversion, developed from the works of Romanowicz and Suárez (1983), consists of using only the spectral amplitudes of the mantle waves, while discarding the phase information which could be affected by timing or location errors. The data space is increased by considering both Rayleigh and Love waves over the frequency window 5–10 mHz. Okal and Reymond (2003) have shown that the method is particularly well suited to historical earthquakes. The absence of the phase information results in a double 180° indeterminacy on strike and slip angles, which can be resolved by using body wave polarities at critical stations. For "pure" mechanisms, such as strike-slip ($\delta = 90°$; $\lambda = 0°$), dip-slip ($\delta = 90°$; $\lambda = \pm 90°$) or pure thrust/normal ($\delta = 45°$; $\lambda = \pm 90°$), the double indeterminacy reduces to a single choice of polarity of the solution. Finally, some centroid depth constraint can occasionally be obtained by optimizing the variance reduction of inversions performed at variable, but constrained, depths.

3. Results

Relocations, focal mechanisms and scalar moments obtained in this study are detailed in Appendix 1, which also documents on Figs. A1–A8

Table 3
Summary of focal mechanisms and seismic moments derived in this study.

Number	Date	Region	Focal mechanism			M_0	Method	Interpretation
			ϕ(°)	δ(°)	λ(°)	(10^{27} dyn cm)		
Interplate thrust								
18	07 Dec 1955	Southern Bonin				~0.3	M_m	Thrust
7	24 Feb 1934	Northern Marianas	144	46	57	2.3	PDFM	Oblique interplate thrust
13	13 Jun 1947	Northern Marianas	103	22	48	0.43	PDFM	Oblique interplate thrust
10	28 Dec 1940	Central Marianas	180	8	97	4.0	PDFM	Interplate thrust
CMT[a]	26 May 1978	Volcano Islands	157	16	66	0.08	CMT	Interplate thrust
Outer rise normal faulting								
12	26 Feb 1945	Bonin Islands	31	50	−98	0.71	PDFM	Outer rise normal faulting
22	27 Oct 1966	Northern Marianas	297	55	−125	0.14	P–M_c	Outer rise normal faulting
CMT[a]	21 Dec 2010	Bonin Islands	110	40	−137	1.8	CMT	Outer rise normal faulting
CMT[a]	05 Apr 1990	Southern Marianas	185	31	−108	1.6	CMT	Outer rise normal faulting
Fore-arc normal faulting								
17	27 Aug 1954	Volcano Islands	176	35	−77	0.86	PDFM	Fore-arc normal faulting
16	01 Feb 1954	Volcano Islands	309	44	−101	0.85	PDFM	Fore-arc normal faulting
14	19 Jun 1947	Northern Marianas	332	45	−80	0.92	PDFM	Fore-arc normal faulting
25	11 May 1974	North-central Marianas	143	58	−80	0.07	P–M_c	Fore-arc normal faulting
3	24 Oct 1930	Central Marianas	106	61	−87	0.87	PDFM	Fore-arc normal faulting
23	01 Sep 1970	Central Marianas	350	63	−80	0.11	P–M_c	Fore-arc normal faulting
15	02 Jul 1949	Southern Marianas	249	51	−80	0.66	PDFM	Fore-arc normal faulting
Other mechanisms								
21	10 Feb 1966	Northern Marianas	355	65	27	0.08	P–M_c	Intra-slab strike-slip
9	17 Jan 1940	Southern Marianas	179	84	−175	2.6	PDFM	Outer rise strike-slip
11	14 Jun 1942	Southern Marianas	244	49	93	0.36	PDFM	Outer rise thrust

[a] Included for reference (and plotted on Fig. 1b and c) are the two largest Global CMT solutions (1990, 2010), and the largest interplate thrust CMT solution (1978), for the whole Bonin-Mariana system.

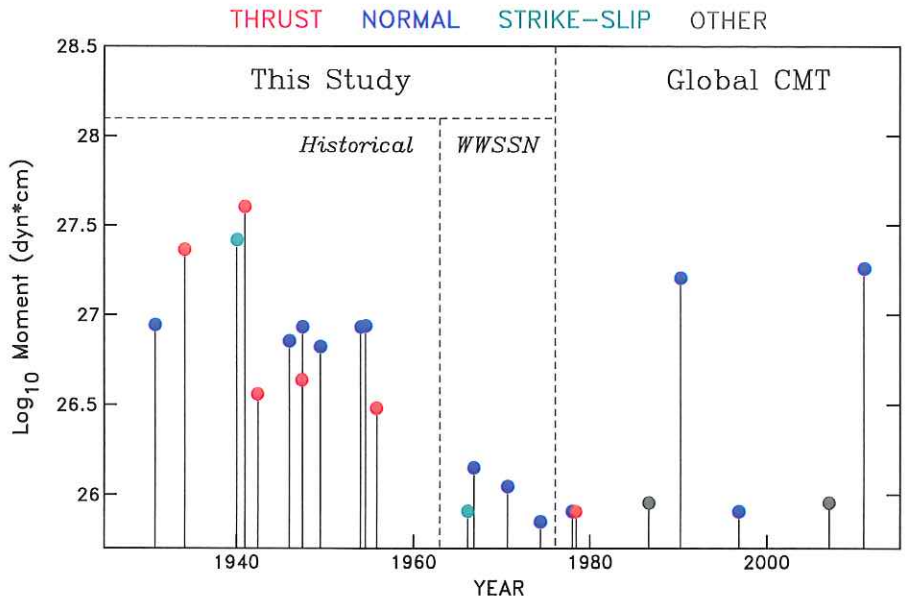

Fig. 2. Timeline of the occurrence of large earthquakes in the Bonin-Mariana subduction system. The earthquakes are color-coded as in Fig. 1. Note the undersampling by the CMT catalog, especially for thrust events.

the most crucial first motions which allowed us to lift the indeterminacy of the PDFM inversions. Table 3 lists all 15 new focal solutions, regrouped according to the nature of the mechanism and its interpretation, with the events listed in order of decreasing latitude inside a given group. The focal solutions are also represented on Fig. 1, where they are color-keyed according to their nature. Fig. 2 summarizes a timeline of the events studied here, together with Global CMT solutions with $M_0 \geq 7 \times 10^{25}$ dyn cm, color-coded for mechanism. It is clear that the digital era (post-1975) grossly undersamples the true level of seismicity of the Bonin-Mariana subduction system, especially regarding thrusting mechanisms.

We emphasize the presence of substantial bathymetric heterogeneities on the Pacific plate, which may affect the subduction process, notably around 16°N, 19°N, 20.5°N, and most significantly off Kita-Iwo-Jima, from 24.7 to 26.5°N. At those locations, the trench does not reach 7000 m (Fig. 1b and c), and it is probable that the stress field in the subducting lithosphere is distorted as a result of the presence of these anomalous structures. We note however that, with the possible exception of the northernmost location off Kita-Iwo-Jima, these areas of potential "choking" of the subduction by bathymetric features do not correlate obviously with the locations of the large earthquakes investigated in the present study.

3.1. Thrust faulting events

We obtain three new solutions (Events 7, 13, 10) whose combined location and thrusting mechanism express interplate thrust corresponding to the subduction of the Pacific lithosphere under the Philippine plate. In addition, it is probable that Event 18 also represents interplate thrusting, although we could not fully resolve its mechanism. All four events have seismic moments from 4 to 50 times larger than the greatest interplate thrust solution of the CMT catalog for our entire study area. This result clearly illustrates the undersampling of the true interplate seismicity of the Bonin-Mariana subduction system by this still young catalog.

In addition, Event 11 constitutes an intriguing case of thrust faulting in the outer rise. It is discussed more at length below.

3.2. Normal faulting events

The majority (9) of our new solutions are normal faulting events, of which only two (Events 12, 22) occurred seawards of the trench in the familiar geometry of normal faulting induced by buckling in the outer rise, while the remaining 7 occur in the fore-arc. This is probably due to the weak expression of the outer rise in this largely decoupled subduction zone (Uyeda and Kanamori, 1979).

3.3. Strike-slip events

The remaining two events feature a strike-slip mechanism. Event 21, a relatively small shock in the fore-arc at 29–42 km depth, has a T axis normal to the local direction of the trench, expressing the generally tensional regime of the fore-arc. Event 9, on the outer slope of the trench, is the third largest solution inverted in this study (and shares with Event 10 the largest magnitude assigned by GR (7.3)). Its interpretation is not straightforward.

3.4. Frequency-moment relations

Fig. 3a shows a frequency-moment regression of recent shallow events with a predominantly thrusting mechanism. The dataset used consists of all shallow (h<100 km) Global CMT solutions (1976–May 2011) in the study area with a P axis dipping less than 45°, a T axis dipping more than 45° and an N axis dipping less than 20°. Fig. 3b shows the same regression for normal faulting events, defined with opposite limits on the P and T axes. The regressions are expressed as

$$\log_{10} N = \alpha - \beta \log_{10} M_0 \quad (2)$$

where the parameter β (Molnar, 1979) is expected to take the exact value 2/3 under the assumption of scaling along a fault zone of fractal dimension 2 (Okal and Kirby, 1995; Rundle, 1989). The normal faulting dataset of 184 events features a rather smoothly varying population whose regression yields $\alpha = 14.91; \beta = 0.55$, significantly less than the theoretical value of 2/3. For the thrust faulting dataset, the smaller population (113 events) features only 4 shocks beyond 10^{25} dyn cm, which restricts a meaningful regression to $M_0 \leq 10^{25}$ dyn cm. The latter ($\alpha = 19.21; \beta = 0.72$) has a slope in better agreement with its theoretical value than for the normal faulting dataset. When these regressions are extrapolated to the 82-yr window spanned by our present study and the CMT era, the values of α become 19.57 for thrust events and 15.28 for normal ones. The former predicts 3 thrust earthquakes of moments $M_0 \geq 3 \times 10^{26}$ dyn cm, the latter 12 normal

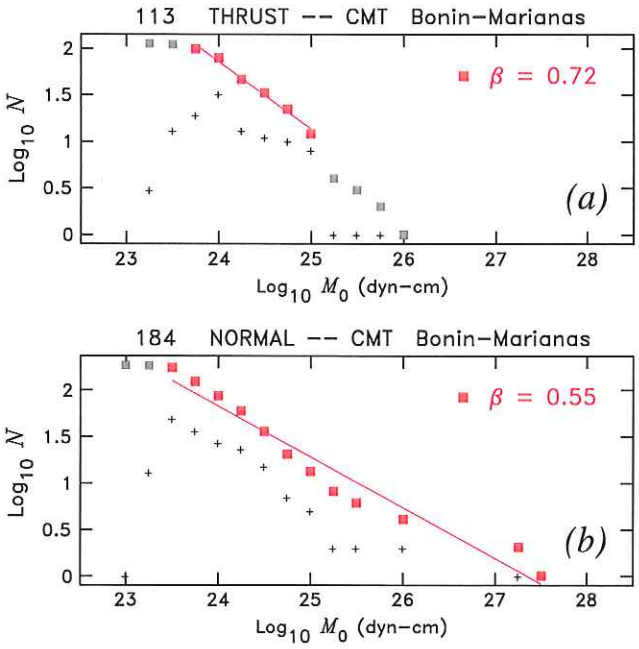

Fig. 3. Frequency–moment statistics for thrust (a) and normal faulting (b) CMT solutions in the Bonin-Mariana subduction system. Small plus signs are individual populations of bins with a width of 0.25 logarithmic unit; the larger symbols are the cumulative populations. The gray symbols in the background are not used in the regressions, which are shown by the straight segments. See text for details.

faulting events with moments $M_0 \geq 7\times10^{25}$ dyn cm, these bounds representing the minimum moment values inverted in the present study, which would suggest that the dataset is complete beyond them. For thrust events, Table 3 contains 5 earthquakes with greater moments, and the Global CMT dataset none. For normal faulting events, there are 9 pre-digital earthquakes in Table 3, and 4 in the Global CMT dataset (including two listed in Table 3), for a total of 13. In both cases, and given the uncertainties inherent in the statistics of small numbers, the observed populations compare favorably with those obtained by extrapolating the statistics of modern populations to a longer time window.

Conversely, the level of seismicity suggested by the population of thrust events would suggest a return period of 320 years for an earthquake of moment 10^{28} dyn cm. In this context, we note that in their authoritative, monumental catalog of tsunamis, Solov'ev and Go (1984) mention two events of interest. In 1872 a "strong earthquake" was followed, at Chichijima, by six or seven waves, while the sea had been calm (Cholmondeley, 1915). Clearly, this event had to be significantly larger than the historical earthquakes listed by GR and studied here, none of which resulted in documented tsunamis. In 1826, a "very strong" earthquake was associated with a 6-m wave at Chichijima. However, the original reference (Beechey, 1831) mentions that this took place during "a tremendous storm," which suggests that the flooding may have been a combination of a typhoon and a local tsunami, and the 6-m figure cannot be definitely interpreted. Nevertheless, the 1872 episode and probably the 1826 one demonstrate that earthquakes even larger than the 20th-century events studied here can occur in the Bonin Islands.

4. The case of Event 11

Event 11 constitutes a rare case of thrusting in the outer rise. This geometry was originally recognized, albeit at a much smaller size ($M_0 = 3.7\times10^{25}$ dyn cm), by Chen and Forsyth (1978) in Tonga, as expressing the release of a compressional bending stress in the lower half of the subducting plate, while the upper half is under tension.

Based mostly on compilations by Stauder (1973, 1975) and Stauder and Mualchin (1976), Chapple and Forsyth (1979) later documented 10 more such events, but they argued that they were obviously rarer than their normal faulting counterparts, and "apparently restricted to a few isolated locations (although this may be an artifact of poor statistics)," namely to five subduction systems: Kuril, Tonga-Kermadec, Chile, Peru and Central America. No seismic moments are available for these earthquakes, but conventional magnitudes are reported as large as $M_s = 7.2$.

A few years later, Christensen and Ruff (1983) proposed that outer rise thrusting could also be controlled by timing within the earthquake cycle, namely that in strongly coupled subduction zones (e.g., Chile), these events would take place towards the end of the seismic cycle when stresses accumulating prior to a large interplate earthquake would put all layers of the oceanic plate under compression. They based their model principally on a large outer rise thrusting event (16 October 1981; $M_0 = 5.1\times10^{26}$ dyn cm) offshore of what was then the Valparaíso seismic gap, which would indeed rupture during the large interplate event of 19 March 1985. Dmowska et al. (1988) then used a computational algorithm for elastic loading during the interseismic cycle to quantify Christensen and Ruff's (1983) model, concluding that outer rise thrust events (as well as tensional ones down-dip from the locked interplate site) could occur typically within the last tenth of the seismic cycle. We emphasize that the models in those two studies applied only to strongly coupled subduction zones. By contrast, in uncoupled subduction zones (of which the Marianas constitute the classic endmember), the *a priori* absence of a locked interface would suppress the concept of a seismic cycle (and of a seismic gap), and outer rise thrust events could occur at any time in Chen and Forsyth's (1978) geometry (Christensen and Ruff, 1983).

Two decades later, an examination of the Global CMT catalog (1976–May 2011) reveals at least 33 more outer rise thrust events (defined as occurring seaward of the outer trench slope), involving a total of 12 subduction zones; only the Bonin-Mariana, Nankai, Ryukyu, Kamchatka and Vanuatu trenches have no clear such solutions during the digital era. The largest earthquake remains the 1981 event in Chile, followed by that of 04 September 1977 off the Kermadec Islands ($M_0 = 1.6\times10^{26}$ dyn cm).

In this context, and in addition to being clearly located in the outer rise with a relatively deep focus (39 km; see Appendix 1 for details), Event 11 features a compressional axis dipping 4° in azimuth 332°, i.e., only 17° away from the azimuth of relative motion of the Pacific and Philippine plates, as computed using Sella et al.'s (2002) REVEL model. Thus, it is an inescapable conclusion that Event 11 forms an additional example of outer rise thrusting. This earthquake is particularly remarkable, being the only such event known in the Bonin-Mariana subduction system, and having a large seismic moment ($M_0 = 3.6\times10^{26}$ dyn cm) falling between the 1981 Chilean and 1977 Kermadec ones. This would suggest that large outer rise events could occur in all subduction zones, not only in the strongly coupled ones. However, it remains difficult to interpret Event 11 in the framework of the model published, for coupled systems, by Christensen and Ruff (1983) and quantified by Dmowska et al. (1988), as it should have been the harbinger of a large interplate shock, which has failed to materialize over the past 70 years, in contrast to its most comparable counterparts in Chile and Kermadec, both of which were followed by large interplate events within a few years. Rather, under Chen and Forsyth's (1978) model, Event 11 appears large, but remains comparable to its normal faulting companion of 05 April 1990, only 120 km to the North (open star on Fig. 1b). This situation would tend to support Christensen and Ruff's (1983) assertion that their time-controlled model would not apply to decoupled subduction systems.

5. Conclusion

The conclusion of this study is that, when properly extended over a sufficiently long time window, the population statistics of thrusting events in the Bonin-Mariana subduction zone are well described by an extrapolation of the modern seismicity. They show no evidence

of magnitude saturation at the level of a "maximum earthquake" of the size expected for thrust events under Ruff and Kanamori's (1980) paradigm, with Event 10 reaching a moment six times larger than predicted under that model. The report of the 1872 earthquake and tsunami (and possibly that of 1826) indicates that earthquakes even larger than recorded instrumentally have occurred in the province, and therefore that they can and will occur in the future, rarely of course, but ineluctably. They should be taken into account when assessing the level of hazard risk of the region, and possibly of other subduction zones lacking known large interplate thrust events.

In this respect, our results lend additional credence to the precautionary suggestion by McCaffrey (2007) and Stein and Okal (2007) that all subduction zones, regardless of their tectonic parameters, may be prone to very large interplate thrust earthquakes, as long as they possess enough length to accommodate the necessary rupture; note that this limitation is largely insignificant, since most if not all subduction zones are longer than the 400-km of rupture documented in the 2011 Tohoku event.

The analysis of Event 11 further indicates that outer rise thrust earthquakes can occur in poorly coupled subduction systems, under Chen and Forsyth's (1978) model, where they can reach large moments without requiring the time-dependent build-up of compressional stresses described in coupled systems under Dmowska et al.'s (1988) model. The maximum size of any such events remains elusive, and thus, their capacity to generate at least a local tsunami cannot be ruled out *a priori*. In particular, this still poorly known class of events should not be discounted when evaluating the sources of regional tsunami hazard, just like their large normal faulting counterparts in the outer rise, which are known to occasionally generate catastrophic tsunamis (e.g., Sanriku, 02 March 1933; Sumbawa, 19 August 1977), in a time frame whose relation to the seismic cycle may be clearly apparent (e.g., Kuril Is., 13 January 2007) or presently still not understood (e.g., Sanriku, 02 March 1933).

Acknowledgments

We are grateful to Ian Saunders (Pretoria), Bernard Dost (De Bilt), Tiar Prasetya (Jakarta), Geneviève Patau (St. Maur), Steve Kirby and James Dewey (USGS) for access to historical seismological archives. We thank the Editor, Dr. Fumiko Tajima, and the anonymous reviewers for their constructive comments and suggestions. Maps were drawn using the GMT software (Wessel and Smith, 1991).

Appendix 1. Detailed results for primary events

Pre-1962 Earthquakes

- Event 3, 24 October 1930, Central Marianas
  This earthquake occurs in the fore-arc, about half-way between the island of Pagan and the trench. We propose a depth of 15 km based on the minimum of location residuals for constrained-depth relocations. EV used a constrained depth of 35 km.
  The PDFM inversion was successful using Rayleigh and Love waves from only two stations, De Bilt (DBN) and Tucson (TUC); it yielded a moment of 8.7×10^{26} dyn cm. Kataseismic first arrivals at DBN, Pasadena (PAS) and especially Hongo (Tokyo; HNG; Fig. A1) then constrain the solution to ($\phi=106°$; $\delta=81°$; $\lambda=-87°$).
- Event 7, 24 February 1934, Northern Marianas
  This earthquake occurs under the fore-arc in the bend between the Volcano and Mariana Islands. Whereas its epicenter is well constrained, its depth is essentially unresolved by the abundant dataset of 136 retained *P* times. We propose a depth of 25 km which minimizes location residuals; EV fixed the depth at 35 km.
  The PDFM inversion uses Rayleigh waves at Abuyama (ABU), DBN, Honolulu (HON), San Juan (SJG) and TUC, yielding a seismic moment $M_0=2.3\times10^{27}$ dyn cm. Strong, impulsive anaseismic *P* arrivals at ABU, DBN and HON, shown on Fig. A2, and an Eastward *S* arrival at HON, rule out a normal faulting solution, and constrain the mechanism to ($\phi=144°$, $\delta=46°$, $\lambda=57°$), giving the solution a strong component of thrust.
- Event 9, 17 January 1940, Southern Marianas
  The floating depth relocation converges on 22 km, at an epicenter located on the outer wall of the trench, about 200 km East of Guguan Island. EV obtained a comparable depth of 31 km. Both these results and the location of the epicenter rule out the deeper focus (80 km) proposed by GR.
  The PDFM inversion uses Rayleigh and Love waves at the four stations DBN, HON, SJG, TUC, and yields a strike-slip mechanism with a moment of 2.6×10^{27} dyn cm. Impulsive first motions at PAS (kataseismic) and HNG (anaseismic) resolve its polarity with a final mechanism of ($\phi=179°$; $\delta=84°$; $\lambda=-175°$).
- Event 10, 28 December 1940, Central Marianas
  The event relocates in the forearc, only 5 km from EV's epicenter. The residuals of depth-constrained relocations show a weak minimum at 30 km; EV imposed a 35 km depth. By contrast, GR suggested 80 km, a figure not supported by our relocation of the dataset available to B. Gutenberg (Goodstein et al., 1980).
  The PDFM inversion uses Rayleigh waves at College (COL), DBN, HON, PAS and SJG, and Love waves at COL, DBN, HON and PAS. It yields a moment of 4.0×10^{27} dyn cm, the largest obtained in this study. We were able to verify an excellent impulsive kataseismic arrival at TUC (see Fig. A3), and an emergent one at Huancayo (HUA). The ISS also lists a generally coherent set of first arrivals, which constrain the solution to ($\phi=180°$; $\delta=8°$; $\lambda=97°$).
- Event 11, 14 June 1942, Southern Marianas
  Both modern relocations (EV: 14.54°N, 148.01°E; this study: 14.53°N, 147.92°E, error ellipse less than 50 km in length) clearly put this event East of the trench (Fig. A4), under the (poorly developed) outer rise. Our epicenter is also similar to the ISS solution (14.5°N;

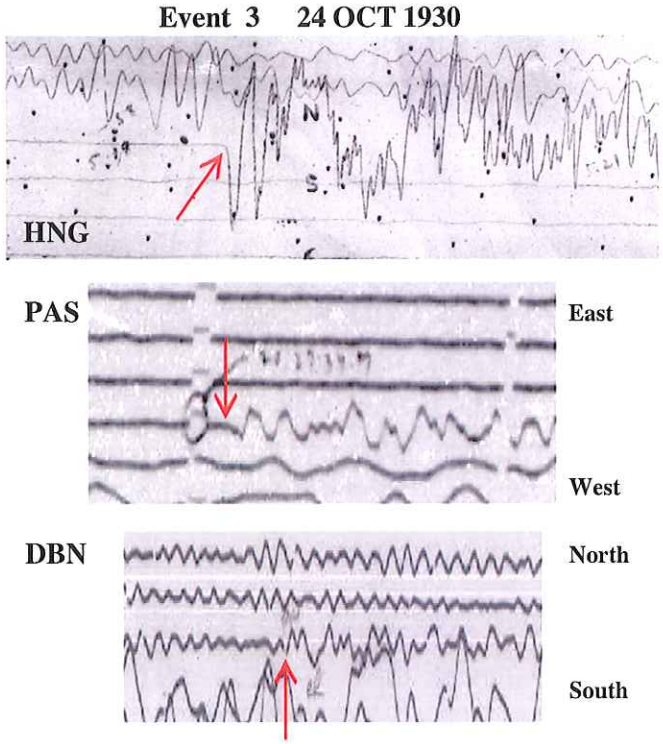

Fig. A1. Close-up of original seismograms for Event 3, showing critical first-motion arrivals used to resolve the indeterminacy of the PDFM algorithm, and to establish the normal-faulting character of the mechanism. Minute marks are shown as dots (HNG), vertical offsets (PAS) or 1-s gaps in recording (DBN). To sharpen the arrivals, the vertical scale of the PAS and DBN records has been multiplied by 2.

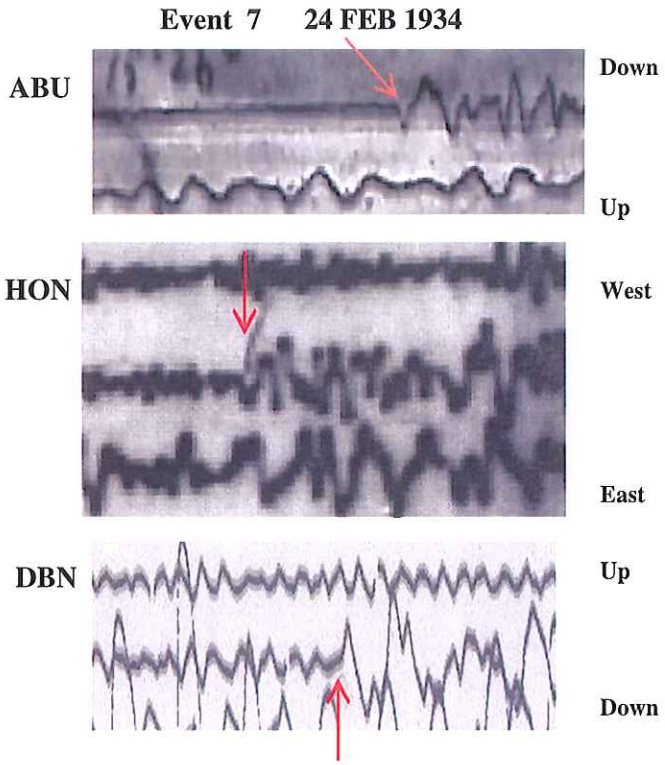

Fig. A2. Same as Fig. 1 for Event 7. The windows shown are 103 (ABU), 125 (HON) and 125 s (DBN) long. Vertical scale multiplied by 2 at ABU and DBN.

148°E). A location on the interplate thrust contact would require a r.m.s. residual of 5.7 s, more than double that at our inverted epicenter. The floating depth relocation converges to $h=39$ km, in good agreement with EV's value of 49 km, with the broad minimum of residuals for constrained relocations (Fig. A4c), and with a delay of 12 s between the impulsive arrivals of *P* and *pP* at PAS (Fig. A4b). The ISS suggests a depth of 65 km, while GR propose 80 km (Goodstein et al., 1980), a figure mistakenly transcribed as 0 in the NOAA database. By contrast, GR locate this earthquake in the back arc at 145°E (solid triangle on Fig. A4a). We attempted to relocate the earthquake using only

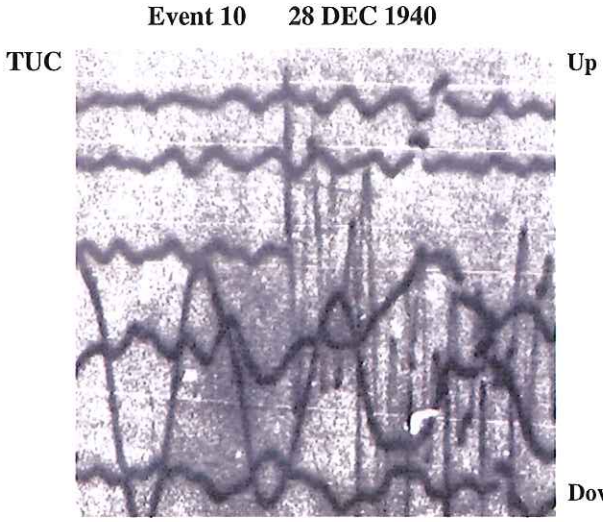

Fig. A3. Vertical record at Tucson for Event 10, establishing normal faulting character of solution. Window is 66 s long.

the dataset recorded in B. Gutenberg's notepads (Goodstein et al., 1980), but it suffers from a lack of near-field stations; regardless of the constrained depth chosen, all solutions converge to 14.1°N, 150.8°E (open triangle with large ellipse on Fig. A4a), 300 km East of our epicenter, and more than 600 km from GR's solution. We must conclude that this event constitutes a rare example of a clearly erroneous location by GR, probably due to their use of a severely depleted dataset. The PDFM inversion uses Rayleigh waves at DBN, HON, PAS and SJG, and Love waves at PAS. It converges on the mechanism ($\phi=244°$; $\delta=49°$; $\lambda=93°$), whose polarity is constrained by two impulsive anaseismic arrivals at PAS (Fig. A4b) and HUA, and an emergent one at HNG. The strike angle is constrained by the emergent nature of the HNG arrival. The inverted moment is 3.6×10^{26} dyn cm.

- Event 12, 26 February 1945, Volcano Islands
  The earthquake relocates 240 km East of Kita-Iwo-Jima Island, near the trench, but in an area where the latter is poorly expressed with a maximum depth of only 5000 m. While it is technically possible to obtain converging floating depth solutions, the latter have depths between 150 and 200 km incompatible with the geometry of the Wadati–Benioff zone, located more than 250 km to the West. We prefer to constrain the depth to a shallow value (20 km), which still gives an acceptable r.m.s. residual (3.3 s). EV did not invert this event; GR propose a depth of 50 km, at an epicenter 51 km NNE of ours.
  The PDFM inversion uses Rayleigh and Love waves at TUC, HON and SJG, and yields a seismic moment of 7.1×10^{26} dyn cm. Kataseismic first motions at TUC (impulsive; Fig. A5) and HUA (emergent), and an emergent anaseismic one at ABU constrain the mechanism to a normal faulting geometry ($\phi=31°$; $\delta=50°$; $\lambda=-98°$).
- Event 13, 13 June 1947, Northern Marianas
  The earthquake relocates under the forearc, along the bend separating the Volcano and Mariana Islands. Our relocations suggest a shallow depth (10 km), based on a monotonous increase of residuals with constrained depth. The earthquake was not relocated by EV.
  We were able to use 5 Rayleigh waves (COL, HON, HUA, PAS, SJG) and 6 Love waves (ABU, COL, HON, HUA, SJG, TUC) in the PDFM inversion, which yields a moment $M_0=4.3\times10^{26}$ dyn cm. Anaseismic first arrivals at ABU and DBN and kataseismic ones at PAS and TUC (emergent; Fig. A6) constrain the solution to the oblique thrust mechanism ($\phi=103°$; $\delta=22°$; $\lambda=48°$). This mechanism also predicts the very strong kataseismic *pP* at PAS, whose time delay supports a depth of 10–15 km. All this evidence suggests an interplate thrust geometry.
- Event 14, 19 June 1947, Northern Marianas
  This earthquake took place six days after the previous one, and relocates only 26 km to the Northwest, again in the fore-arc. Residuals for constrained depth relocations are minimal at 30 km. The event was not relocated by EV.
  The PDFM inversion uses Rayleigh waves at COL, DBN, HON and TUC, and Love waves at DBN, COL and HON. It yields a moment of 6.5×10^{26} dyn cm. Kataseismic first motions at PAS, TUC and Vladivostok (VLA) define a normal faulting mechanism ($\phi=332°$; $\delta=45°$; $\lambda=-80°$), the opposite strike (152°) being also acceptable; it would rotate the mechanism only 14° in the formalism of Kagan (1991).
- Event 15, 02 July 1949, Southern Marianas
  The earthquake relocates in the forearc, in the vicinity of the trench, East of Sarigan and Anatahan Islands. A shallow depth is suggested by the monotonous increase of constrained-depth solutions with depth. GR fixed the depth at 50 km, and EV did not relocate the event.
  The PDFM inversion was performed on Rayleigh and Love waves at DBN and TUC, yielding a moment of 6.6×10^{26} dyn cm. Impulsive kataseismic records at PAS, TUC and DBN constrain its geometry to normal faulting ($\phi=249°$, $\delta=51°$, $\lambda=-80°$).
- Event 16, 01 February 1954, Volcano Islands
  The earthquake relocates at the toe of the forearc, 200 km East of Minami-Iwo-Jima Island. Residuals for constrained-depth relocations have a weakly pronounced minimum at 40 km, in agreement with EV's fixed depth of 46 km.

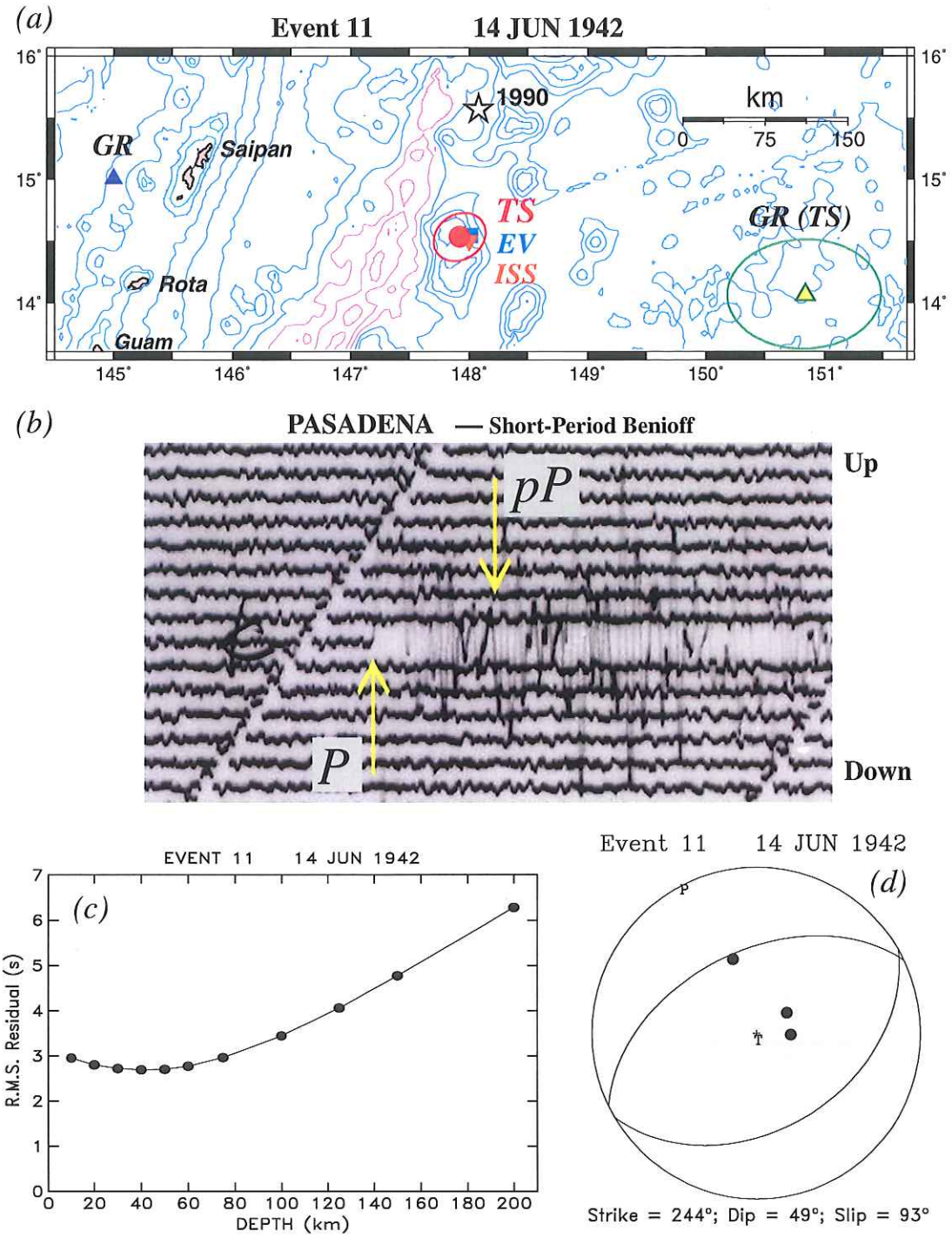

Fig. A4. (a): Close-up of the relocation of Event 11, as determined in this study ("TS"; solid dot with small error ellipse). The location is essentially identical to EV's (square) and the ISS solution (inverted triangle). The solid triangle shows GR's location, more than 300 km to the West, and the open triangle (with large ellipse), our relocation of their dataset, 300 km to the East of the preferred solution ("GR (TS)"). The star shows the large 1990 normal faulting event nearby. Bathymetric contours as in Fig. 1. (b): Close-up of *P* and *pP* arrivals at Pasadena. Note the impulsive anaseismic *P*, and the time delay of *pP*, suggesting a depth of 45 km. (c): RMS residuals as a function of depth for constrained relocations, featuring a broad minimum around 40 km. (d): Final focal mechanism inverted by PDFM, and constrained by first-arrival polarities.

The PDFM inversion, based on Rayleigh waves at DBN, SJG, HON and TUC, and Love waves at SJG, TUC and DBN, yields a moment of 8.5×10^{26} dyn cm. The normal faulting character of the event is established by a sharp impulsive kataseismic arrival at PAS (Fig. A7), and supported by numerous reports of kataseismic arrivals at teleseismic distances in the ISS. We select the solution ($\phi=309°$, $\delta=44°$, $\lambda=-101°$); the strike indeterminacy cannot be lifted, but the two possible solutions are rotated only 16° from each other in the formalism of Kagan (1991).

- Event 17, 27 August 1954, Volcano Islands

  This earthquake relocates about 30 km to the West of the previous one, in the fore-arc. It is not listed in EV's catalog. The floating depth relocation converges on a very shallow solution (4 km), but the dataset has essentially no depth resolution, with a flat residual curve for constrained depth inversions, down to 50 km. The ISS proposes a depth of 64 km.

  The PDFM inversion uses Rayleigh waves at DBN, HON and PAS, and Love waves at DBN, and yields a moment of 8.6×10^{26} dyn cm. A lone

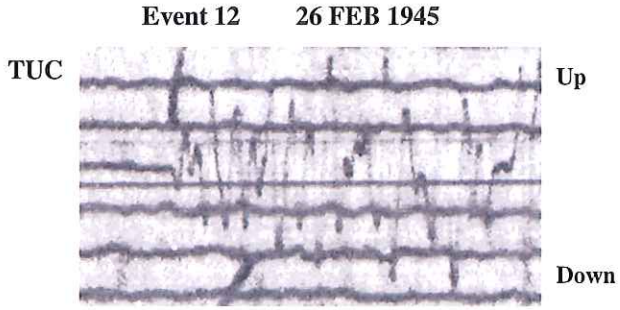

Fig. A5. Same as Fig. 3 for Event 12. Window is 27 s long.

kataseismic arrival at PAS constrains the solution to normal faulting. We propose the focal mechanism ($\phi = 176°$; $\delta = 35°$; $\lambda = -77°$); the strike indeterminacy cannot be lifted, with the two possible solutions rotated 26° from each other in the formalism of Kagan (1991).

- Event 18, 07 December 1955, Bonin Islands
  The earthquake relocates at the forearc, in the proximity of Hahajima Island. It was not relocated by EV. We propose a depth of 25 km, which provides a weak minimum of residuals, but note that the dataset has practically no depth resolution.
  Records at DBN could not be used because of an interruption in the recording during the arrival of mantle waves. As a result, the PDFM inversion, based on Rayleigh waves at HON and PAS and Love waves at SJG and PAS, failed to converge. In the absence of a definitive focal mechanism, we propose a moment on the order of 3×10^{26} dyn cm, based on an average mantle magnitude $M_m = 6.5 \pm 0.4$ (Okal and Talandier, 1989)
  A lone, emergent anaseismic first arrival at PAS suggests a component of thrust in the focal mechanism; this earthquake could represent interplate motion at the subduction interface.

Post–1962 Earthquakes: The WWSSN Era

- Event 21, 10 February 1966, Northern Marianas
  This event occurs inside the slab, at a depth of 42 km [EV]. A dataset of 35 *P*-wave first motions constrains the mechanism to a strike-slip geometry (Fig. A8). Spectral amplitudes in the 100–200 s range yield $M_c = 5.88$ or $M_0 = 7.6 \times 10^{25}$ dyn cm, with a trend towards slowness.
- Event 22, 27 October 1966, Northern Marianas
  This event is located near the trench, at a shallow depth (9 km, according to EV). A dataset of 32 *P*-wave first motions polarities constrain the focal geometry to a predominantly normal mechanism (Fig. A8). Spectral amplitudes grow regularly with period, indicating slowness in the source, with a moment at 200 s on the order of 1.4×10^{26} dyn cm. The normal faulting character of the earthquake suggests that it represents bending of the plate in the vicinity of the trench.

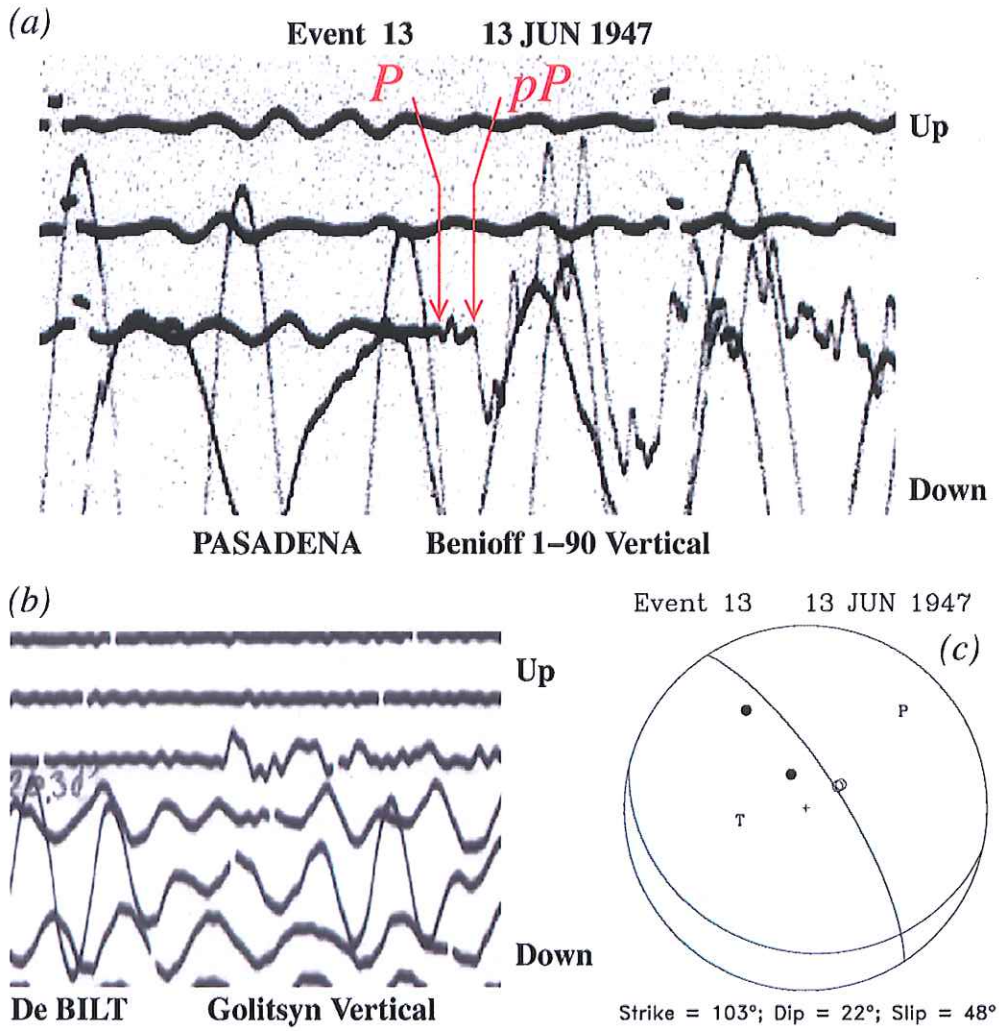

Fig. A6. (a) Close-up of Benioff 1–90 vertical record of Event 13 at PAS. Note kataseismic arrivals of *P* (emergent) and *pP* (impulsive, with much larger amplitude). (b): *P* arrival at DBN; vertical scale multiplied by 2. (c): Final mechanism inverted by PDFM and constrained by first motions.

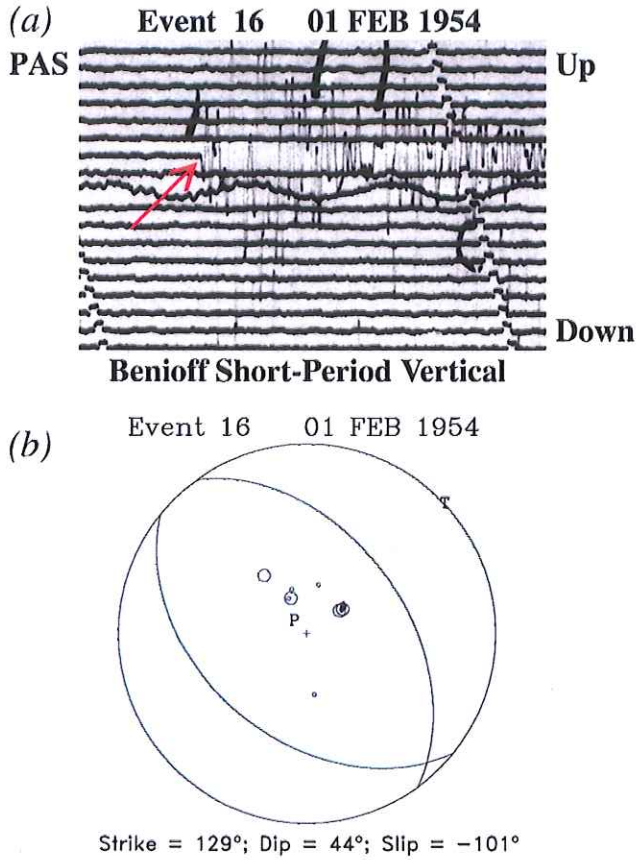

Fig. A7. (a): Close-up of short-period vertical record of Event 16 at PAS. (b): Final mechanism, inverted by PDFM with polarity determined by first arrivals. On this figure, the larger symbols were read as part of this study, the smaller ones are reported by the ISS.

- Event 23, 01 September 1970, Central Marianas
  This event is located in the slab, at a depth of 60 km (EV). It features a normal faulting mechanism, perfectly constrained by a dataset of 37 *P*-wave first motions (Fig. A8). Spectral amplitudes yield a moment of 1.1×10^{26} dyn cm, with no significant growth with period.
- Event 24, 11 May 1974, North-Central Marianas
  This earthquake locates in the fore-arc, immediately West of the trench. A dataset of 38 *P*-wave first-motion polarities strongly constrains the focal geometry to a normal faulting mechanism with tension across the trench (Fig. A8). The corrected magnitudes M_c show a slight growth with period, which could suggest a trend towards source slowness. The average value of the resulting moment is $M_0=6.3\times10^{25}$ dyn cm.

Appendix 2. Ancillary Events

- Event 1, 23 March 1913
  Expectedly, this earthquake is rather poorly constrained, but all fixed-depth relocations place it arc-wards of the trench. Residuals feature a broad minimum for a depth of 150 km, which would place the event inside the slab. This depth is significantly greater than proposed by GR (80 km); the earthquake was not relocated by EV. A preliminary investigation based on the polarity of *P* and *S* waves at Tokyo and Irkutsk (IRK), and on the spectral amplitudes of Rayleigh and Love waves at Tokyo would be generally compatible with $M_0=1.3\times10^{27}$ dyn cm in the geometry ($\phi=320°$; $\delta=90°$; $\lambda=30°$). This value of the moment would also agree with $M_{PAS}=7.0$, as published by GR, and with the fact that the earthquake was recorded only as traces on the Wiechert instrument at Göttingen (GTT).
- Event 2, 24 November 1914
  This event was given an exceptionally high magnitude (8.7) in the NOAA Geophysical Database, which was then transcribed *verbatim* by Båth and Duda (1979), and later EV, as a "Pasadena magnitude". However, GR give only $M=8.1$, which can be verified on Gutenberg's original notepads (Goodstein et al., 1980).
  Remarkably, a floating-depth relocation based on 18 *P* arrival times converges on a hypocenter at 371 km, with $\sigma=5.5$ s, an excellent figure for the 1910s. By contrast, GR proposed 110 km; the ISS did not comment on the depth. An examination of generalized SKS/S phases on the Golitsyn records at De Bilt confirms an epicentral depth of 350–400 km, which coincides (at that latitude) with the maximum depth of the seismogenic zone, as defined for example by EV's catalog. We note that the earthquake was felt in Guam, 1000 km away.
  Estimates of mantle magnitudes (Okal, 1990) were computed from the HNG and DBN records, yielding $M_m=7.6$ (HNG) and 8.2 (DBN) for Rayleigh waves and 8.2 (HNG and DBN) for Love waves. These values can be reconciled with a mechanism such as ($\phi=230°$; $\delta=30°$; $\lambda=155°$) which also agrees with the *P* and *S* polarities observed at HNG and DBN. The corrected magnitude becomes $M_c=8.01\pm0.3$, or $M_0=10^{28}$ dyn cm, larger than any CMT solution known in this depth range, both in the Bonin-Marianas and elsewhere (Fiji, 11 July 1992; Honshu, 01 January 1984).
  The inspection of B. Gutenberg's notepad for the event reveals that he had difficulty assigning a depth and a magnitude to the event, as evidenced by numerous corrections and crossed out entries. Most of his magnitude estimates were derived from *P* and *S* waves (as would be expected from an event at 370 km depth, but not necessarily from a shallower one at 110 km), for which the relationship between the magnitude scale derived by Gutenberg (1945) and the modern concept of moment lacks a firm theoretical basis. At any rate, an examination of the correction factor $A(\Delta,h)$ for body wave magnitudes indicates that the use of GR's lesser depth would result in an overestimation of the magnitude by 0.1 to 0.5 units, depending on distance, and on the exact iteration of the amplitude correction *A* (Gutenberg, 1945 vs. Gutenberg and Richter, 1956) used in that particular computation. Perhaps significantly, it is worth noting that B. Gutenberg had originally assigned a lesser value of "about 7…?" (later crossed out and not fully legible on the pad), but which could be $7\frac{1}{2}$ or $7\frac{3}{4}$, before crossing it out and replacing it with 8.1. In all cases, we fail to find any justification for the value of 8.7 entered as a Pasadena magnitude in the NOAA database, and surmise that it must be the result of a clerical error.
  The tentative conclusion of this preliminary study of the 1914 shock is that it may represent a very large but certainly not gigantic shock at the bottom of the seismogenic zone in that segment of the subduction system. Any further study, which would warrant the use of more historical seismograms, would be beyond the scope of the present paper.
- Event 5, 09 September 1931
  This event is well constrained, with the residuals minimized at a depth of 120 km, placing the source perfectly inside the slab, although shallower than EV's relocation at 173 km. GR assume a surficial source.
- Event 8, 01 January 1938
  The floating depth relocation converges to a depth of 77 km, confirming GR's estimate of 80 km. By contrast, EV imposed a default depth of 35 km. Our hypocenter locates along the inferior boundary of the slab.
- Event 19, 29 November 1956
  The floating depth relocation converges to 65 km, although this figure is poorly constrained. However, the event is clearly in the back-arc, and is not considered further in this study. It was not included in EV's catalog.
- Event 20, 31 October 1960
  Arrival times are not listed in the ISS, which during the years 1957–1962 only lists phase times from selected, sufficiently large earthquakes. It is not listed by EV. However, a dataset of 14 *P* times is reported in the Bulletin of the Bureau Central International de

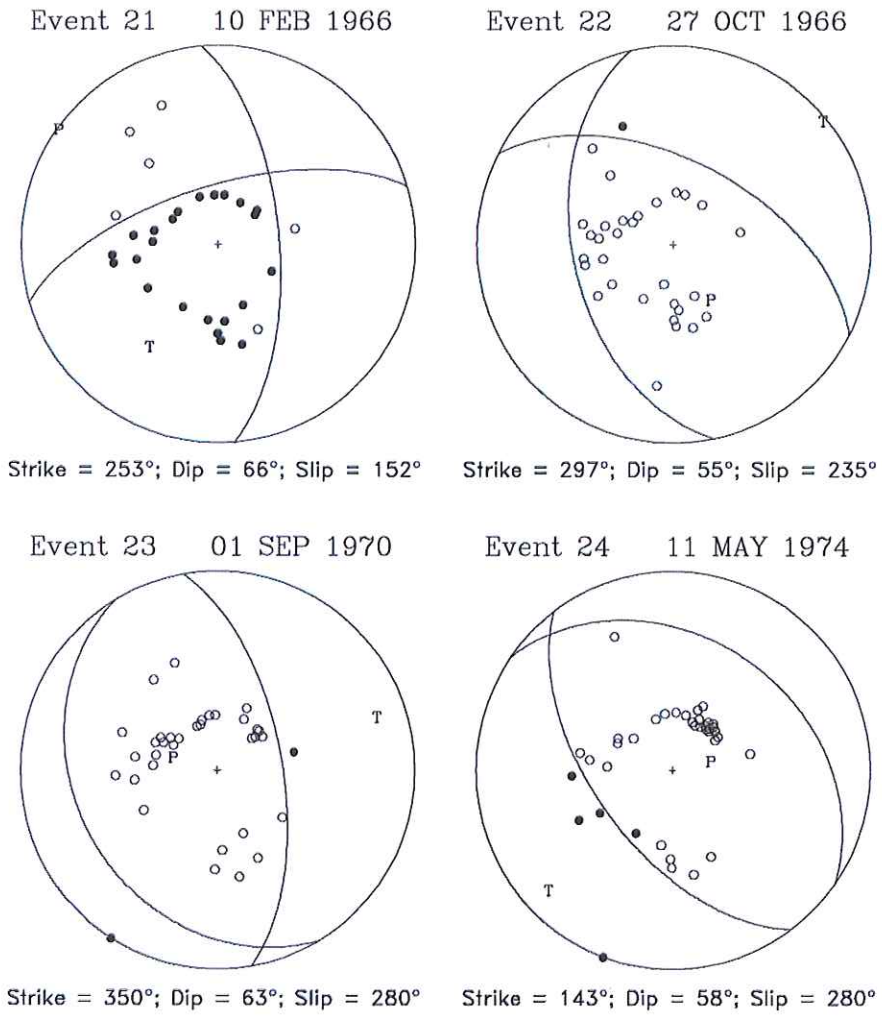

Fig. A8. Focal mechanisms for Events 21–24, obtained from first motion *P*-wave polarities read on WWSSN seismograms.

Séismologie (Strasbourg). A floating depth relocation converges on 42 km, but has essentially no depth resolution since Monte Carlo floated depths with σ_G as small as 1 s (which is the precision of the reported times) range from 0 to 325 km. On the other hand, the epicenter is robustly located only 40 km East of Minami-Iwo Jima, indicating that the earthquake cannot be an interplate event.

References

Båth, M., Duda, S.J., 1979. Some Aspects of Global Seismicity, Report I–79. Univ. Uppsala.

Beechey, F.W., 1831. Narrative of a Voyage to the Pacific and Beering's Straits. Colburn and Bentley, London. 742 pp.

Bird, P., 2003. An updated digital model of plate boundaries. Geochemistry, Geophysics, Geosystems 4 (3) (GC000252, 52 pp.).

Chapple, W.M., Forsyth, D.W., 1979. Earthquakes and bending of plates at trenches. Journal of Geophysical Research 84, 6729–6749.

Chen, T., Forsyth, D.W., 1978. A detailed study of two earthquakes seaward of the Tonga Trench: implications for mechanical behavior of the oceanic lithosphere. Journal of Geophysical Research 83, 4995–5003.

Cholmondeley, L.B., 1915. The History of the Bonin Islands. Constable & Co, London. 178 pp.

Christensen, D.H., Ruff, L.J., 1983. Outer-rise earthquakes and seismic coupling. Geophysical Research Letters 10, 697–700.

Dmowska, R., Rice, J.R., Lovison, L.C., Josell, D., 1988. Stress transfer and seismic phenomena in coupled subduction zones during the earthquake cycle. Journal of Geophysical Research 93, 7869–7884.

Engdahl, E.R., Villaseñor, A., 2002. Global seismicity: 1900–1999. In: Lee, W.H.K., Kanamori, H., Jennings, P.C., Kisslinger, C. (Eds.), International Handbook of Earthquake and Engineering Seismology. Academic Press, pp. 665–690.

Goodstein, J.R., Kanamori, H., Lee, W.H.K., 1980. Seismology microfiche publications from the Caltech archives. Bulletin of the Seismological Society of America 70, 657–658.

Gutenberg, B., 1945. Magnitude determination for deep-focus earthquakes. Bulletin of the Seismological Society of America 35, 117–130.

Gutenberg, B., Richter, C.F., 1954. Seismicity of the Earth and Associated Phenomena. Princeton Univ. Press . 310 pp.

Gutenberg, B., Richter, C.F., 1956. Magnitude and energy of earthquakes. Annali di Geofisica 9, 1–15.

Kagan, Y.Y., 1991. 3-D rotation of double-couple earthquake sources. Geophysical Journal International 106, 709–716.

McCaffrey, R., 2007. The next great earthquake. Science 315, 1675–1676.

Molnar, P., 1979. Earthquake recurrence intervals and plate tectonics. Bulletin of the Seismological Society of America 69, 115–133.

Müller, R.D., Roest, W.R., Royer, J.-Y., Gahagan, L.M., Sclater, J.G., 1997. Digital isochrons of the world's ocean floor. Journal of Geophysical Research 102, 3211–3214.

Okal, E.A., 1990. M_m : a mantle wave magnitude for intermediate and deep earthquakes. Pure and Applied Geophysics 134, 333–354.

Okal, E.A., Hartnady, C.J., 2009. The South Sandwich Islands earthquake of 27 June 1929: seismological study and inference on tsunami risk for the South Atlantic. South African Journal of Geology 112, 359–370.

Okal, E.A., Kirby, S.H., 1995. Frequency-moment distribution of deep earthquakes: implications for the seismogenic zone at the bottom of slabs. Physics of the Earth and Planetary Interiors 92, 169–187.

Okal, E.A., Reymond, D., 2003. The mechanism of the great Banda Sea earthquake of 01 February 1938: applying the method of preliminary determination of focal mechanism to a historical event. Earth and Planetary Science Letters 216, 1–15.

Okal, E.A., Talandier, J., 1989. M_m: a variable period mantle magnitude. Journal of Geophysical Research 94, 4169–4193.

Okal, E.A., Borrero, J.C., Synolakis, C.E., 2006. Evaluation of tsunami risk from regional earthquakes at Pisco, Peru. Bulletin of the Seismological Society of America 96, 1634–1648.

Rees, B.A., Okal, E.A., 1987. The depth of the deepest historical earthquakes. Pure and Applied Geophysics 125, 699–715.

Reymond, D., Okal, E.A., 2000. Preliminary determination of focal mechanisms from the inversion of spectral amplitudes of mantle waves. Physics of the Earth and Planetary Interiors 121, 249–271.
Romanowicz, B.A., Suárez, G., 1983. An improved method to obtain the moment tensor depth of earthquakes from the amplitude spectrum of Rayleigh waves. Bulletin of the Seismological Society of America 73, 1513–1526.
Ruff, L.J., 1989. Do trench sediments affect great earthquake occurrence in subduction zones? Pure and Applied Geophysics 129, 263–282.
Ruff, L.J., Kanamori, H., 1980. Seismicity and the subduction process. Physics of the Earth and Planetary Interiors 23, 240–252.
Ruff, L.J., Kanamori, H., 1983. Seismic coupling and uncoupling at subduction zones. Tectonophysics 99, 99–117.
Rundle, J.B., 1989. Derivation of the complete Gutenberg–Richter magnitude-frequency relation using the principle of scale invariance. Journal of Geophysical Research 94, 12337–12342.
Scholl, D.W., Kirby, S.H., Keranen, K.M., Wells, R.E., Blakely, R.J., Michael, F., von Huene, R., 2007. Megathrust slip and the care and feeding of the subduction channel through which the seismogenic zone runs. EOS Transactions of the American Geophysical Union 88 (52) (T51E-06 (abstract)).
Scholl, D.W., Kirby, S.H., Keranen, K.M., Blakely, R.J., Wells, R.E., 2010. Confirmation that large-magnitude megathrust earthquakes are linked to the subduction of thick, laterally continuous bodies of trench sediment. EOS Transactions of the American Geophysical Union 91 (52) (T22B-08 (abstract)).
Sella, G.F., Dixon, T.H., Mao, A., 2002. REVEL: a model for recent plate velocities from space geodesy. Journal of Geophysical Research 107 (B4) (ETG_11, 32 pp.).
Solov'ev, S.L., Go, Ch.N., 1984. Catalogue of tsunamis on the Western shore of the Pacific Ocean. Canadian Translation Fish Aquatic Sciences 5077 (439 pp.).
Stauder, W.J., 1973. Mechanism and spatial distribution of Chilean earthquakes with relation to subduction of the oceanic plate. Journal of Geophysical Research 78, 5033–5061.
Stauder, W.J., 1975. Subduction of the Nazca plate under Peru as evidenced by focal mechanism and by seismicity. Journal of Geophysical Research 80, 1053–1064.
Stauder, W.J., Mualchin, L., 1976. Fault motion in the larger earthquakes of the Kurile–Kamchatka arc and the Kurile–Hokkaido corner. Journal of Geophysical Research 81, 197–308.
Stein, S., Okal, E.A., 2005. Size and speed of the Sumatra earthquake. Nature 434, 581–582.
Stein, S., Okal, E.A., 2007. Ultra-long period seismic study of the December 2004 Indian Ocean earthquake and implications for regional tectonics and the subduction process. Bulletin of the Seismological Society of America 97, S279–S295.
Stein, S., Engeln, J., Wiens, D., Fujita, K., Speed, R., 1982. Subduction seismicity and tectonics in the Lesser Antilles arc. Journal of Geophysical Research 87, 8642–8664.
Tsai, V.C., Nettles, M., Ekström, G., Dziewoński, A.M., 2005. Multiple CMT source analysis of the 2004 Sumatra earthquake. Geophysical Research Letters 32 (17) (17304, 4 pp.).
Uyeda, S., Kanamori, H., 1979. Back-arc opening and the mode of subduction. Journal of Geophysical Research 84, 1049–1061.
Wessel, P., Smith, W.H.F., 1991. Free software helps map and display data. EOS Transactions of the American Geophysical Union 72, p441, 445–446.
Wysession, M.E., Okal, E.A., Miller, K.L., 1991. Intraplate seismicity of the Pacific Basin, 1913–1988. Pure and Applied Geophysics 135, 261–359.